EXTENDING THE *HSRI* TYRE MODEL FOR LARGE INFLATION PRESSURE CHANGES

Höpping, Kristian; Augsburg, Klaus; Büchner, Florian

TU Ilmenau, Department of Mechanical Engineering, Automotive Engineering Group

ABSTRACT

The choice of the optimal tyre inflation pressure is always a conflict of aims since the inflation pressure has a significant influence on safety, comfort and environmental behaviour of a vehicle. The development of a dynamic Tyre Pressure Control System (TPCS) can reduce the conflict of minimal rolling resistance and maximal traction. Driven by the requirements for autonomous driving, recently substantial progress was made to predict the road conditions precisely and robust. This premise moves the development of a Tyre Pressure Control System (TPCS) to the focus of research.

To study the influence of the tyre inflation pressure on longitudinal tyre characteristics under laboratory conditions, an experimental sensitivity analysis is performed using a multivalent usable Corner Module Test Rig (CMTR) developed by the Automotive Engineering Group at Technische Universität Ilmenau. The test rig is designed to analyse suspension system and tyre characteristics on a roller of the recently installed 4 chassis roller dynamometer. Camber angle, toe angle and wheel load can be adjusted continuously. In addition, it is possible to control the temperature of the test environment between -20°C and +45°C. The results of the experimental study, that covers a wide range of different wheel loads and inflation pressures for three different tyre variations, show a significant influence of the inflation pressure on longitudinal tyre characteristics as slip stiffness or maximum traction force. To simulate the influence of a TCPS on vehicle dynamics with a numerical simulation tool, it is essential to describe the influence of the inflation pressure on tyre characteristics correctly with a tyre simulation model. Consequently, the well-known physically based *HSRI* tyre model adapted from *Dugoff* is extended for large inflation pressure changes. The model parameters for the tyre model are determined with a parameter identification method implemented in a developed automatic *MATLAB* analysis tool. The extended *HSRI* tyre model shows a good model accuracy to represent the tyre inflation pressure dependent tyre characteristics.

Index Terms – tyre inflation pressure, *HSRI* tyre simulation model

1.   INTRODUCTION

To reach the ambitious goal of lowering CO_2 emissions of passenger cars reducing the rolling resistance of tyres is becoming a stronger focus of research. New tyre dimensions, novel tyre designs and an increased inflation pressure are promising approaches to reduce the rolling resistance significantly. [1, 2] Regarding the rolling resistance forces of a tyre it is well known that a higher tyre inflation pressure leads to decreased rolling resistance losses and consequently to a lower fuel consumption, respectively lower emissions (see [3, 4, 5]). Decreasing the rolling resistance by around 30 % results in a 5 % lower fuel consumption, respectively CO_2 emission. [6] A 10 percent reduction in rolling resistance will yield a 1 to 2 percent increase in vehicle fuel economy. [7] According to [3], a 10 % decreased rolling resistance coefficient can be

caused for example by inflating the tyre from 2.1 bar to 2.7 bar. Unfortunately, an increased tyre inflation pressure can reduce traction forces of a tyre. Different publications (see [8, 9, 10]) show the influence of tyre inflation pressure on the stopping distance of a vehicle. *Hadrys et al.* [8] for example measured, that the stopping distance beginning at an initial velocity of 60 km/h can change from 22 meters to 24.6 meters on dry road and from 25.4 m to about 29 meters on wet road when changing the tyre pressure from 2 bar to 3 bar at the front axle. Experimental investigations performed by the authors with different types of vehicles show that the stopping distance can be reduced when changing the inflation pressure (see [11, 12, 13]). Especially on wet road surfaces this effect can be significant. Experiments carried out with a compact car test vehicle on a wet tiled low grip track show that the braking distance could be reduced by around 20 percent when changing the tyre inflation pressure from 3.5 to 1.5 bar. [12] In addition to the influence on rolling resistance losses and stopping distance, tyre inflation pressure has significant effects on vehicle handling dynamics, comfort or tyre wear. Consequently, the right choice of the optimal inflation pressure is always a conflict between the priorities. Car manufacturers propose to adjust the pressure according to the vehicle load. In addition, some manufacturers recommend to deflate the tyres to enhance the comfort at lower speeds and inflate the tyres to drive at higher velocities.

To reduce the conflict of minimal rolling resistance losses and maximal traction force, Tyre Pressure Control Systems (TPCS) were developed in the past. A good overview of available systems is given by [14]. Most of the known Tyre Pressure Control Systems were designed for off-road, military and agricultural ground vehicles to increase traction on rough terrain. However, the dynamic to realize an inflation pressure difference is very limited. Moreover, the desired inflation pressure has to be set by the driver. The benefits of the application of a TPCS for passenger cars were tested with a test vehicle and published by *Skoff* in [15]. Unfortunately, the dynamic of the system was still too slow to realize effects on an emergency braking manoeuvre. Hence, an essential improvement for the application of a TPCS in passenger cars can be achieved through an intelligent controlled system with a high dynamic. Such an automated controlled and highly dynamic Tyre Pressure Control System was proposed by the authors (see [16]). To evaluate the potential of a highly dynamic TPCS on fuel consumption and vehicle dynamics, different calculations were analysed using the numerical simulation tool *IPG CarMaker*. Later, the simulation results were validated with experimental results carried out with a demonstrator vehicle where a highly dynamic TPCS was implemented (see [11]). To simulate the influence of deflating or inflating tyres during the driving manoeuvre a simple lookup table tyre model with a first order transient approach was parameterized from experimental data. As well known, lookup tables are not universally usable for many different operating points. Moreover, a lookup table tyre model with many data points can have a large size and therefore the real time capability or the exchange of data using a standard file format is very limited. Consequently, it is more appropriate to use a common standard tyre model. Various publications, e. g. [17-19], compare different tyre simulation models with each other and present which models are used by researchers of car manufacturers depending on the simulation goal. A very good accuracy as well as a short calculation time for vehicle handling simulations for on-road conditions is given by semi-empirical tyre models. A very prevalent and well-known model, which is supported by many simulation tools, is the *Magic Formula* tyre model. An extension of the model to cover large inflation pressure changes has been presented by the authors in [20]. Due to the limited computing power of electronic control units in vehicles, simpler tyre models are used to estimate certain parameters with observers. A common model for this application is the *HSRI* tyre model (see [21-28]). In this regard, the presented study has the goal to propose a method to extend this tyre model and to parameterize it with test rig experiments.

Using the Corner Module Test Rig (CMTR) developed by the *Automotive Engineering Group* at *Technische Universität Ilmenau*, the tyre inflation pressure influence on longitudinal tyre characteristic curves was analysed for 3 different tyres at 4 different loads and 7 inflation pressures between 1.0 bar and 4.0 bar. The analysed data is used to extend the *HSRI* tyre model for large inflation pressure changes. The extension of the model is described below.

2. EXPERIMENTAL ANALYSIS

2.1 Experimental Procedure

First, the influence of the tyre inflation pressure on longitudinal tyre characteristics is analysed. Therefore a multivalent usable Corner Module Test Rig (CMTR) was developed by the *Automotive Engineering Group* at *Technische Universität Ilmenau.* The test rig is designed to analyse suspension system and tyre characteristics on a roller of the recently installed 4 chassis roller dynamometer. Figure 1 presents a CAD model of the Corner Module Test Rig installed at the rear right roller of the roller chassis dynamometer.
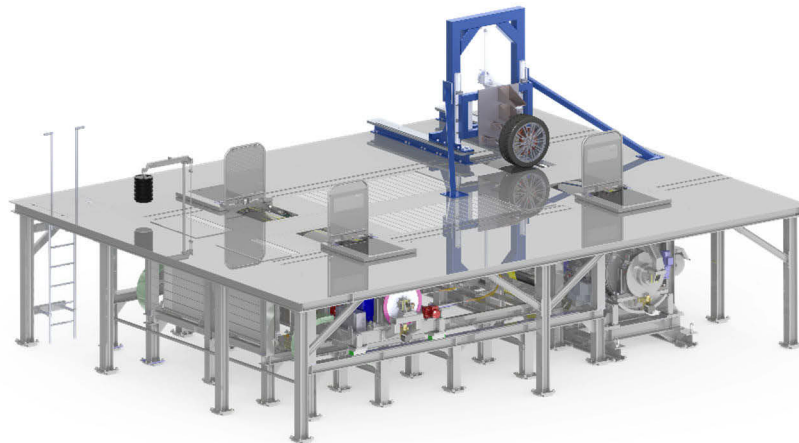

Figure 1: CAD model of Corner Module Test Rig (CMTR) at rear right roller of roller chassis dynamometer

The test rig allows to perform experiments under laboratory conditions. For example, the ambient temperature can be adjusted between -20 °C and +45 °C. Table 1 presents an excerpt of the specifications of the 4 roller chassis dynamometer.

Table 1: Specification of 4 roller chassis dynamometer

Diameter of rollers at front axle	48" (around 1,22 m)
Diameter of rollers at rear axle	75" (around 1,91 m)
Maximum power of motors at front axle	228 kW
Maximum power of motors at rear axle	260 kW
Maximum longitudinal force at front axle	8922 N
Maximum longitudinal force at rear axle	5706 N
Maximum wheel load per roller	1250 kg
Maximum speed	250 km/h
Ambient temperature	-20 °C to +45 °C

To analyse the influence of the tyre inflation pressure on longitudinal tyre characteristics, a modern multi-link chassis system of a mid-range vehicle is connected to frame of the test rig. Camber angle, toe angle and wheel load can be adjusted continuously. To realize brake slip, an

electric servo-hydraulic brake system was designed. A hydraulic disc brake can be actuated by a master brake cylinder. The brake cylinder is actuated by a hydraulic piston. Position and actuation speed is controlled by a servo valve. The developed nonlinear P controller to adjust the brake pressure, and respectively the brake slip, is implemented to the existing data acquisition and control system of the roller chassis dynamometer. Therefore a developed *MATLAB Simulink* control model is compiled and implemented to the *AVL PUMA* and *AVL InMotion* infrastructure. Additional sensors, as brake pressure, speed or temperature sensors, are connected to the F-FEMs (Fast-Front End Modules) to acquire further signals with the *AVL PUMA* data acquisition and control system. To evaluate forces and moments at the test wheel, a *Kistler RoadDyn S635* wheel force transducer is mounted at the CMTR. To compute the actual slip of the wheel, incremental position encoders are installed at the wheel and the roller. The slip angle of the tyre is computed by a signal provided by a laser line scanner. In addition, temperature sensors monitor the actual temperature of the brake disc, the brake fluid and the surface of the tyre tread. Figure 2 presents the Corner Module Test Rig installed at the rear right roller of the chassis roller dynamometer.
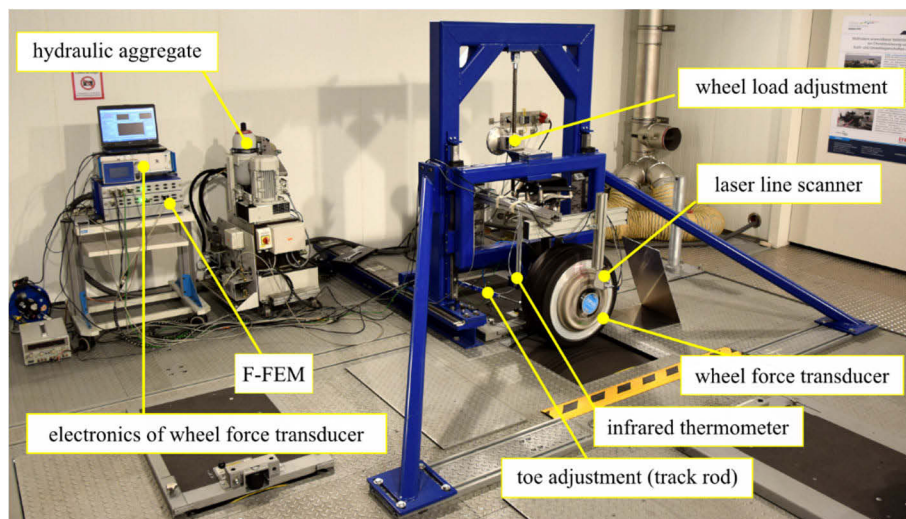

Figure 2: Corner Module Test Rig installed at rear right roller of roller chassis dynamometer

Analogously to established test procedures to gather a longitudinal brake slip vs. friction force coefficient curve, a linear brake pressure ramp with a gradient of 10 bar/s was applied with the brake system. The speed of the roller was kept constant. In this study, the velocity of the roller surface was 50 km/h. To protect the tyre against extended wear, the brakes are released when a brake slip of about 30 % is realized. Consequently, a full dataset is acquired in 5 to 8 seconds (depending on the wheel load). To generate reliable and confident results, every measurement for a specific inflation pressure and wheel load is repeated 3 times. In addition, a warm-up procedure where the tyre runs 30 minutes constantly at a constant speed of 50 km/h followed by 10 braking procedures, was performed before each tyre is analysed. All tests were performed with an active air conditioning system which controlled the temperature and humidity of the ambient air at constant values of 20 °C and 45 % relative humidity. A preliminary study confirmed a very good repeatability of the measurement results. The root-mean-square error (RMSE) of the peak friction value between the 3 measurements is usually under 2 %. The RMSE value of the slip stiffness between the single measurements performed for each inflation pressure and load is only at a very few exceptional cases over 3 % and can be regarded as very small.

As a first step, the inflation pressure influence on longitudinal tyre characteristics is analysed for 3 different tyres on the 48" drum at four different loads (~3000 N, ~3600 N, ~4200 N and

~4800 N) and 7 different inflation pressures (1.0 bar, 1.5 bar, 2.0 bar, 2.5 bar, 3.0 bar, 3.5 bar and 4.0 bar). Table 2 presents an overview of the investigated tyres.

Table 2: Specification of analysed test tyres

	eco tyre	**sports tyre**	**SUV tyre**
manufacturer	Michelin	Michelin	Pirelli
Label	Energy Saver	Pilot Sport 2	Scorpion Verde
application	summer	summer	all-season
dimension	215/55 R 17	235/35 R 19	235/55 R 19
load index	94	87	105
speed index	H	Y	V
DOT	2812	1512	3515
thread depth	ca. 5 mm	ca. 5 mm	ca. 5 mm
Shore A hardness	66.7	72.0	69.7

2.2 Data Processing

Using *MATLAB*, an analysis tool, has been developed to evaluate the measured data automatically. First, the recorded data is converted to a readable data format. Relevant data is extracted. To obtain an appropriate brake slip vs. friction coefficient characteristic curve, a slip classification is applied. In addition, a robust locally weighted regression is applied to smooth the curve slightly. The achieved data can be saved in a standard TYDEX format for further processing (see [29]). In addition, characteristic values as longitudinal slip stiffness, optimal slip, maximum friction force coefficient or RMSE values are calculated. These values are used for the parameter identification technique as initial values. Figure 3 presents the sum of the measured raw data of 3 measurements and the calculated regression curve for the sports tyre from table 2.
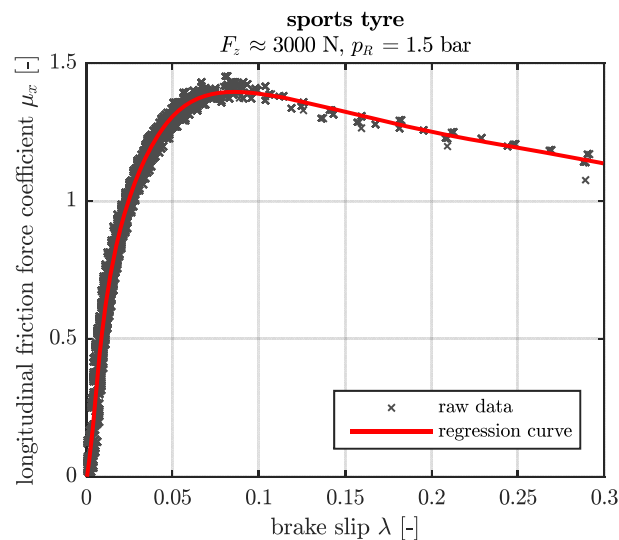

Figure 3: Example of raw data and regression curve of a friction force coefficient characteristic curve plotted against the brake slip

2.3 Experimental Results

2.3.1 Longitudinal friction force coefficient vs. brake slip characteristic

Using the developed *MATLAB* analysis tool, different characteristics as the brake slip - friction coefficient curves can be calculated and plotted. Figure 4 presents the friction force coefficient characteristic plotted against the brake slip for the analysed tyres at a wheel load of around 3000 N for 7 different inflations pressures from 1.0 bar to 4.0 bar. It can be seen that the

inflation pressure has a significant influence on the shape of the tyre curve. In addition, characteristic values from the brake slip - friction coefficient curves are calculated with the *MATLAB* analysis tool. From the literature different values are known that describe the characteristic of tyres. In this study, the longitudinal slip stiffness, the maximum friction force coefficient, the optimal slip and ratio between the maximum friction force coefficient and the friction force coefficient at 30 % brake slip were found appropriate to describe the influence of the inflation pressure on quasi-static longitudinal tyre characteristics.
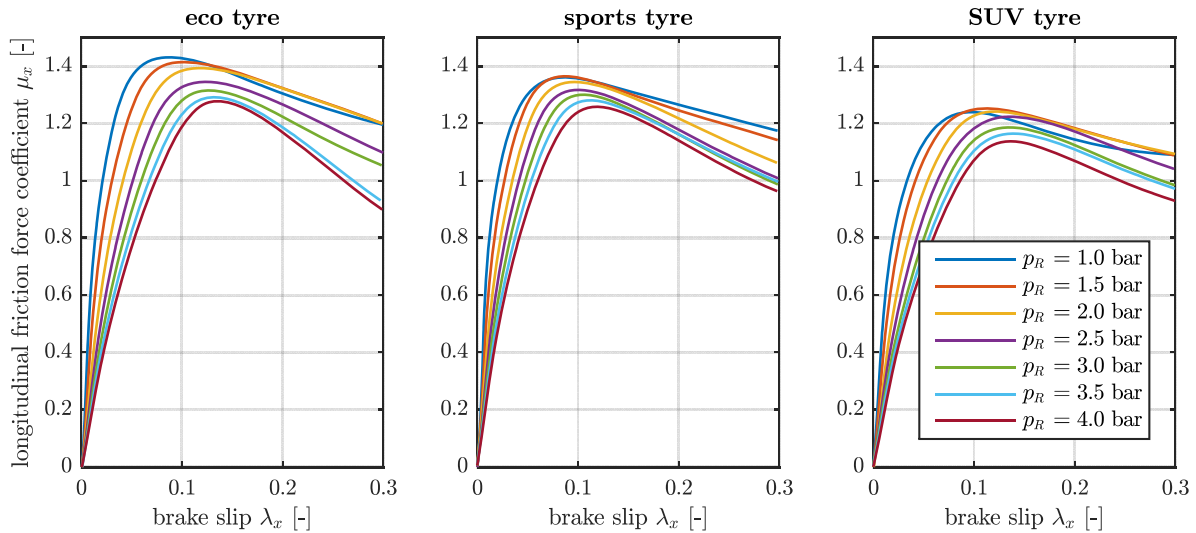

Figure 4: Inflation pressure influence on friction force coefficient vs. brake slip tyre characteristic curve of analysed tyres

2.3.2   Longitudinal slip stiffness

An important characteristic value of a brake slip vs. friction coefficient curve is the longitudinal slip stiffness. The slip stiffness is often calculated as the gradient at zero-crossing. Since with the Corner Module Test rig only brake slip can be generated, another definition is necessary. In literature, it can often be found that at small values of slip the relation between friction force and slip can be regarded as linear. According to [30], the relation between brake slip and friction force coefficient can be assumed to be linear up to a slip of 3 %. Consequently, it is possible to calculate the stiffness with a linear regression using the data of the regression curve up to a slip limit which was defined in this study with 1.5 %. The calculated values depending on wheel load and inflation pressure are illustrated in Figure 5. As expected, the overall slip stiffness values of the low section sports tyre are higher than the mean values of the softer SUV all-season tyre.

As well known, a larger wheel load leads to a higher stiffness. Moreover, it can be seen that there is a large, nonlinear influence of the inflation pressure. Especially at lower inflation pressures, a small change in inflation pressure leads to a large change in slip stiffness. From a first look a quadratic dependency on the tyre inflation pressure can be expected. This can be explained with the tyre footprint length. Regarding a tyre brush model, the longitudinal slip stiffness depends on the tread element stiffness and the contact length. [31] A higher load and a lower tyre inflation pressure result in a larger contact length and consequently in a higher slip stiffness. Regarding the sports tyre at a load of about 4200 N, the stiffness is increased by around 89 % when deflating the tyre from 2.5 bar to 1.5 bar. Moreover the slip stiffness is reduced by about 34 % when inflating the tyre from 2.5 bar to 4.0 bar.
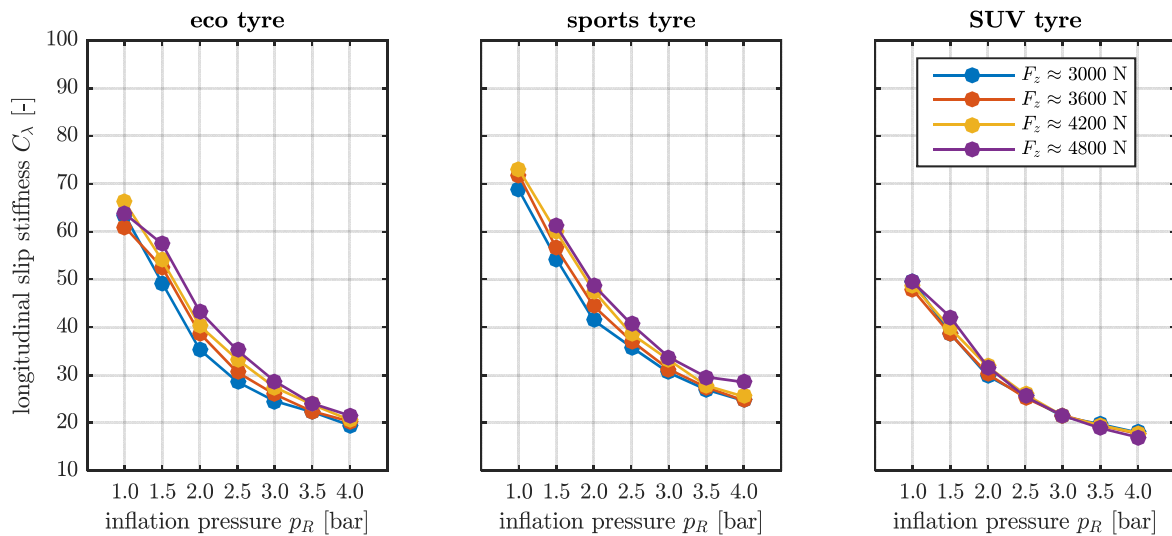
Figure 5: Longitudinal slip stiffness depending on load and inflation pressure

2.3.3 Peak friction force coefficient value

Figure 6 illustrates the maximum calculated longitudinal friction coefficient of the three analysed tyres. As know from the literature, it can be seen that a lower wheel load leads to a higher friction force coefficient. The exception that can be seen for the sports tyre at a load of 3000 N is due to the reason that this measurement took place at two different measurement days. In addition, a light sawtooth tread pattern against the rolling direction due to preliminary test was detected before the experiments at 3000 N. Moreover, it can be seen that the inflation pressure has a significant influence on the maximum longitudinal friction force coefficient. Regarding for example the characteristic curve of the SUV tyre gathered at a wheel load of about 4200 N, the maximum difference of the friction coefficients can be up to 0.114, respectively increased by 10.3 % when deflating the tyre from 4.0 bar to 1.5 bar. Furthermore, it can be noticed that there is - depending on the tyre and the specific load - a maximum peak value depending on wheel load before this tendency changes. Usually, these effects can be explained with the contact pressure distribution. A lower tyre inflation pressure results in a larger contact patch area and a lower pressure distribution. According to the rubber theory, a lower contact pressure increases the transferable traction force on dry roads. When the tyre inflation pressure becomes very small the uniform contact pressure distribution disappears and local pressure peaks will occur. Consequently, the transferable friction force decreases. The peak longitudinal friction coefficient of all analysed tyres show a clear dependency on the inflation pressure. The optimum tyre inflation pressure depends on the tyre itself and the load. To realize the highest friction coefficient, in this study the optimum inflation pressure is between 1.5 to 2.0 bar.
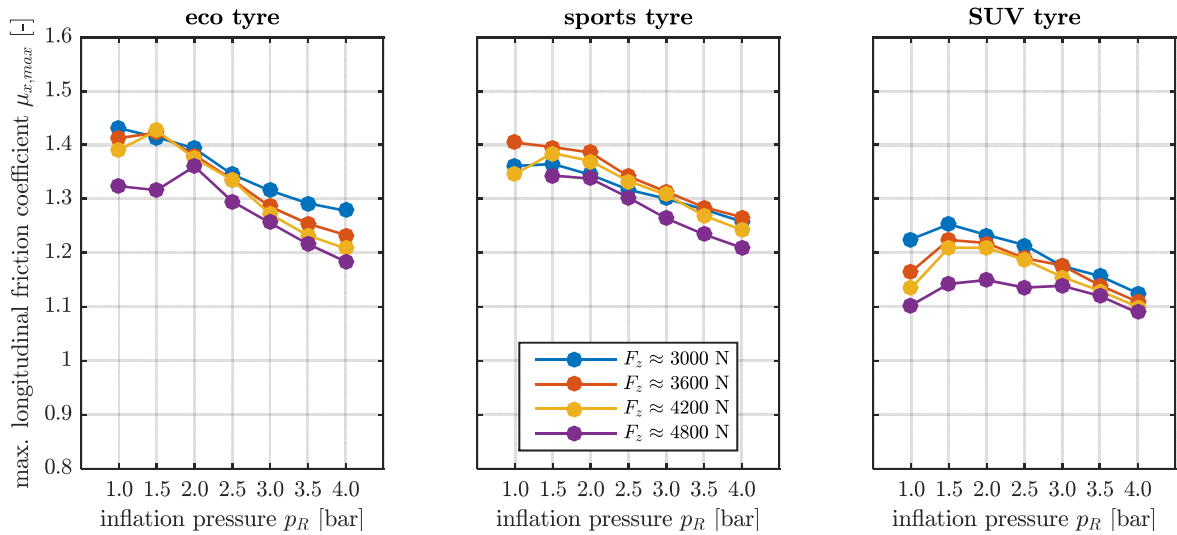
Figure 6: Maximum longitudinal friction force depending on wheel load and inflation pressure

2.3.4 Optimal slip value

Figure 7 presents the optimal slip value at which the peak friction coefficient occurs depending on load and inflation pressure. The value correlates with the slip stiffness and is a crucial factor for the ABS algorithm of a vehicle. The characteristics show that there are minor influence of the load and a significant influence of the tyre inflation pressure on the optimal slip value. The characteristic shows for all analysed tyres that the optimal slip increases with inflating the tyre. Since an increased inflation pressure results in a smaller contact length, the mean deflection and consequently the mean shear stress of the brush elements of the tyre is reduced. To transmit a constant high friction force with a reduced contact length, the deflection of the elements and subsequently the slip of the tyre will increase. The quantitative values of the optimal slip depend on the tyre itself. For the sports tyre at a load of about 4200 N the optimal slip rises from 8.1 % to 11.2 % when increasing the inflation pressure from 1.0 bar to 4.0 bar, whereas the same value rises from 6.8 % to 14.8 % when inflating the eco tyre from 1.0 bar to 4.0 bar at a load of about 4200 N.
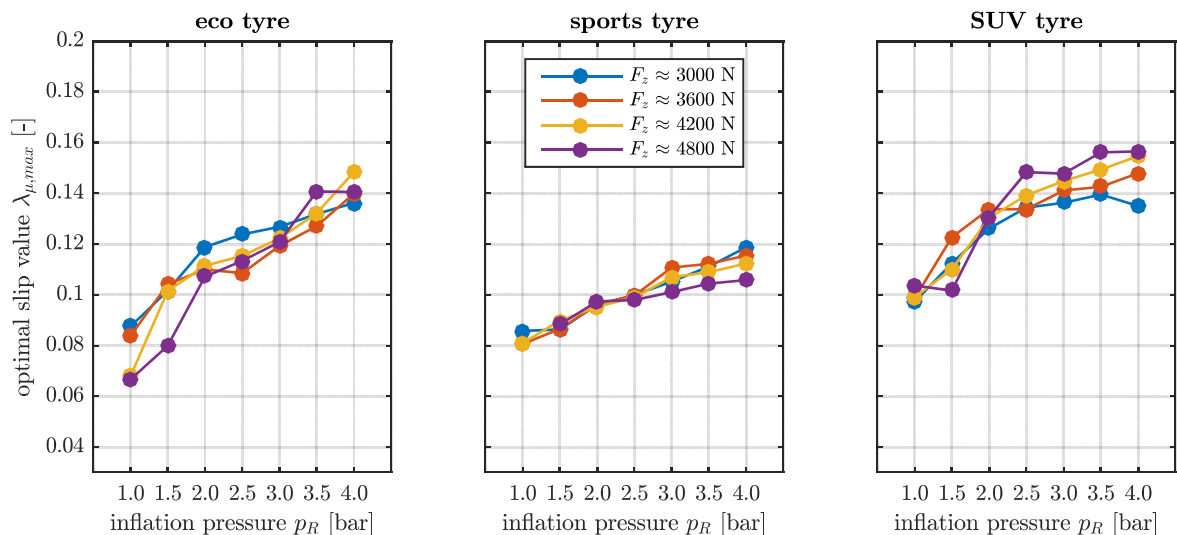

Figure 7: Optimal slip value at peak longitudinal friction

2.3.5   Ratio between peak friction coefficient and friction coefficient at high slip

Figure 8 presents the ratio between the maximum friction force coefficient and the friction force coefficient at 30 % brake slip. Outliers from the expected trend line can be explained with the fact that the values at high slip are obtained in a very short time. Hence, the tyre characteristic curve is only based on a few values and consequently, outliers can influence the pathway of the curve significantly. However, the results show an influence of the tyre inflation pressure on the ratio between peak friction coefficient and friction coefficient at high slip. Although the influence is not significant (e.g. for the sports tyre, the ratio is between 86 % and 93 % for all analysed loads and pressures), the results do not show a clear tyre independent relation. Regarding the sports tyre, the ratio becomes smaller with an increasing inflation pressure, whereas the ratio of the eco tyre and the SUV tyre rises when increasing the tyre inflation pressure.
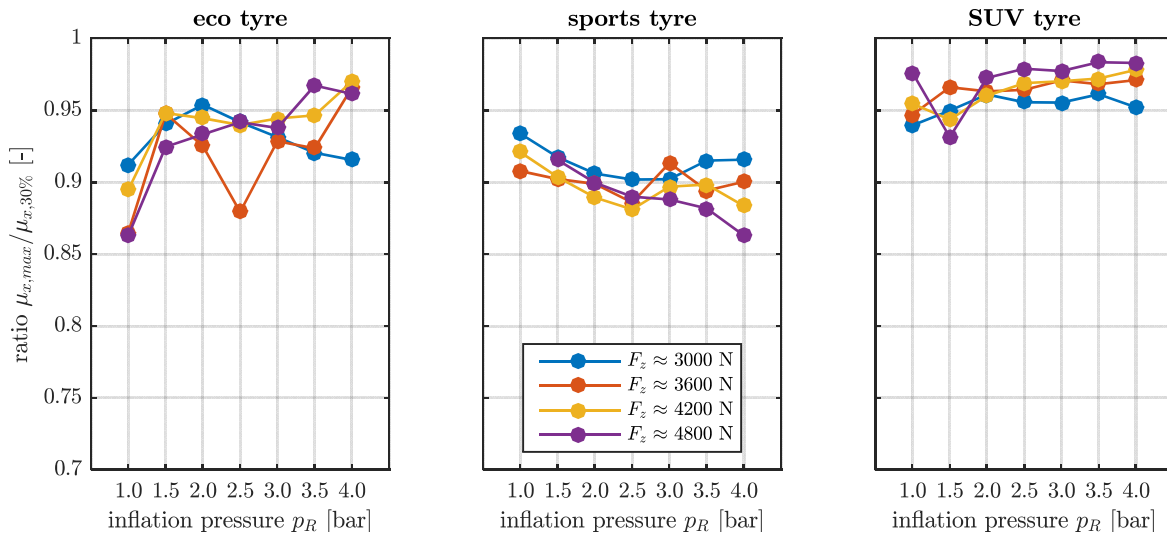

Figure 8: Ratio between peak friction coefficient and friction coefficient at high slip

3.   EXTENDING THE *HSRI* TYRE MODEL

3.1   The basic *HSRI* tyre model

The physically based *HSRI (Highway Safety Research Institute)* tyre model has first been introduced by *Dugoff, Fancher and Segel* [32] in 1969 to calculate the longitudinal and lateral force at a tyre. The authors suggested to regard the section of adhesion and the section of combined adhesion and sliding separately from each other. The forces are calculated from the deformation of the contact patch. Assuming a constant contact pressure distribution, the deformation is regarded as trapezoidal. A suggestions to improve the model was made by *Bernard* et al. [33]. *Wiegner* [34] extended the model to calculate the aligning moment. *Uffelmann* [35] later proposed an improvement to consider wheel load undulations.

The basic equation to calculate the longitudinal force can be written as (see [20, 36-38]):

$$F_x = C_{F\lambda} \cdot \frac{\lambda}{1 + \lambda} \cdot f(K_D) \tag{1}$$

Using the input parameters slip λ, slip angle α, maximum friction coefficient μ_{max} and the load F_z, the dimensionless variable K_D and the function $f(K_D)$ can be calculated. If K_D is larger than 1, no sliding exists. If K_D is smaller than 1, adhesion and sliding occurs in the contact patch area.

$$K_D = \frac{\mu_{max}\, F_z(1+\lambda)}{2\sqrt{(C_{F\lambda}\lambda)^2 + (C_\alpha \tan\alpha)^2}} \tag{2}$$

$$f(K_D) = \begin{cases} K_D(2 - K_D) & if\ K_D < 1 \\ 1 & if\ K_D \geq 1 \end{cases} \tag{3}$$

Due to the small number of coefficients of the tyre model, the computational effort is very low. Consequently the model is especially used in vehicle internal control units to estimate e. g. forces at the tyres (see [21-28]). Compared to the well-known *Magic Formula* tyre model, the approximation accuracy of the measured tyre characteristics is worse. Especially the decreasing tyre force after the maximum traction force at the optimal slip value cannot be represented with the *HSRI* tyre model. Hence, *Bian* et al. [36] suggested in 2014 to multiply the longitudinal friction force F_x with a correction coefficient G_λ as an extension to improve the model accuracy.

$$G_\lambda = (1{,}15 - 0{,}75\mu_{max})\lambda^2 - (1{,}63 - 0{,}75\mu_{max})S + 1{,}27 \tag{4}$$

However, this modification seems not to be valid for a wide variation of tyres. Another promising modification was proposed by *Ding* and *Taheri* [22]. Based on the idea of the *UA* tyre model introduced by *Gim* [39], the actual friction coefficient is calculated from the static friction coefficient μ_p and the sliding friction coefficient μ_s depending on the slip λ.

$$\mu_{mod} = \mu_p - (\mu_p - \mu_s) \cdot \lambda \tag{5}$$

The benefits of this modification can be seen at Figure 9. The friction force coefficient vs. brake slip tyre characteristic curve is clearly better represented by the introduced modification by *Ding* and *Taheri*. Especially, the decreasing behaviour behind the maximum friction coefficient can be described. Hence, the modified model is used to identify the parameters of the basic tyre model and forms the basis for the inflation pressure extensions presented below.
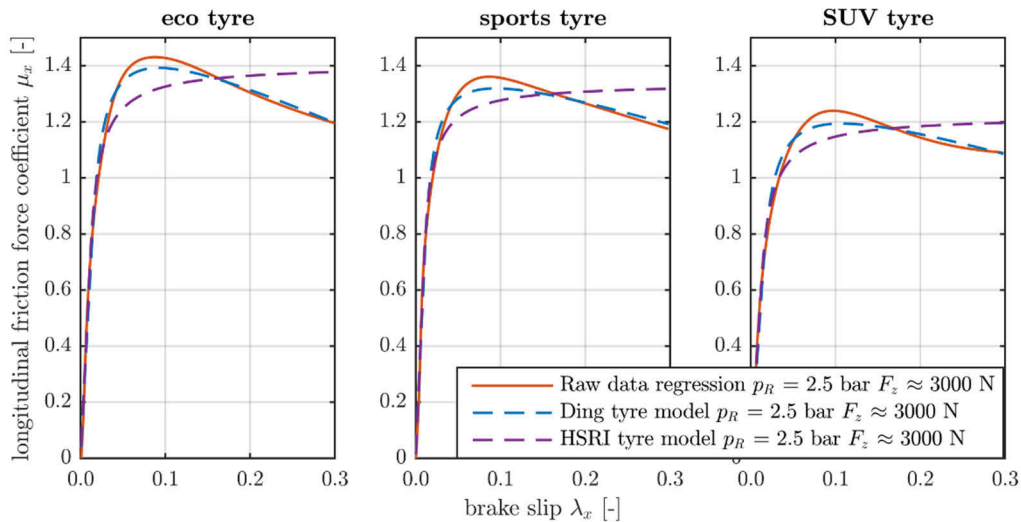

Figure 9: Comparison of the model accuracy between the original HSRI tyre model and the modification by Ding and Taheri

3.2 Parameter identification of tyre model parameters

3.2.1 Identification method of basic model parameters

Different parameter identification methods are known to identify the coefficients of a tyre model. *Van Oosten* and *Bakker* [40] for example presented a software in 1992 to retrieve the parameters of a *Magic Formula* tyre model. A regression method of least squares was applied to obtain the tyre model parameters from measured data. *Schuring, Pelz* and *Pottinger* have also automated the process to obtain the parameters of the *Magic Formula* model and presented it in publication [41]. *Ortiz, Cabrera* et al. presented a new optimization algorithm based on genetic techniques as an alternative method to determine tyre model parameters. [42-43] *Alagappan* et al. [44] compared six different algorithms to fit the *Magic Formula* tyre model with each other. They recommend three algorithms which give good fits for all tested cases by the authors. Furthermore, they recommend to compare the results of a number of algorithms before taking a decision for a specific algorithm.

To identify the basic model parameters of *HSRI* tyre model, different parameter identification algorithms have been implemented to the developed analysis tool using the *MATLAB* Optimization Toolbox (see [45]). A downhill-simplex method adapted from *Nelder-Mead*, a nonlinear regression method adopted from *Levenberg* and *Marquardt*, an interior-point method, a trust-region-reflective technique and a genetic algorithm have been implemented. To guarantee small fit errors and suitable calculation times for the iterative, numerical parameter identification methods, an appropriate objective function as well as convenient bound constraints and termination conditions need to be defined. Depending on the smallest fit error, the appropriate method is applied to identify the basic model parameters.

3.2.2 Enhancement of tyre model equations for large inflation pressure variations and identification of additional parameters

First, all parameters of the basic *HSRI* tyre model are determined separately for every operating point with the above described parameter identification process. Using this data, the parameters for the tyre inflation pressure and wheel load dependencies are determined. This is not done separately from each other. Instead, the calculated initial points of all individual characteristic values are combined in a characteristic array. Thus, the required parameters are determined using an entire parameter identification procedure. Consequently, the parameters of the basic model are used at reference or nominal inflation pressure and load (usually the middle of the analysed values, in this study 2.5 bar and 3.600 N). The inflation pressure and load influence is described by additional terms and parameters. Since the basic *HSRI* tyre model is not able to represent the influence of the tyre inflation pressure, a new approach to cover large inflation pressure changes (and a wide range of loads) had to be found.

Hoogh, Schmeitz et al. [46-47] extended the *Magic Formula* model for small inflation pressure changes in 2005. *Veld, Besselink* et al. [48-49] later extended the *MF-Swift* model by the inflation pressure influence. The results of the research works were taken into account for latest version of the *Magic Formula* model published by *Pacejka* [50] in 2012 and the commercial *MF-Tyre* model version 6.1 [51-52]. The tyre model describes the tyre inflation pressure influence on the longitudinal slip stiffness and on the longitudinal friction coefficient with a second order term. *Höpping, Augsburg* and *Büchner* [20] extended the *Magic Formula* tyre model for large inflation pressure changes, i. a. by introducing pressure depended terms to describe the shape factor and the curvature factor. Due to the limited computing power of internal electronic control units in vehicles, simpler tyre models are often used to estimate certain parameters with observers. A common model for this application is the *HSRI* tyre model (see [21-28]). In this regard, a method to extend this tyre model is presented below.

The experimental results above show clearly that the slip stiffness C_λ and the maximum friction force coefficient $\mu_{x,max}$ are influenced by the inflation pressure. Hence, relations to represent the inflation pressure dependency on the coefficients need to be find. Various functions (e. g. a linear, a quadratic, a cubic and an exponential approach) have been examined in regard of their suitability to represent the measured characteristic curves with appropriate fitting results. Hence, the resulting fit errors for the three analysed tyres were evaluated. In this study second order polynomials were found appropriate to describe the wheel load and inflation pressure dependencies of the three parameters static friction force coefficient μ_p, sliding friction force coefficient μ_s and longitudinal slip stiffness C_λ. This approach delivers good fitting results with a manageable number of coefficients. In some cases the accuracy could be increased by using a third polynomial degree to represent the inflation pressure influence. Since this is not always the case and the number of coefficient rises, these approaches were not followed up. Furthermore, in this study a good model accuracy could be achieved by introducing a quadratic dependency on the load. However, the increase of the fit error is small when using a linear approach. Consequently, a linear dependency on the load could be used, too. Moreover, implementing a parameter, that describes the linear combination of inflation pressure and load (e. g. μ_{pPx1}), increased the accuracy of the extended tyre model distinctly. Since the smallest fitting errors were achieved with the trust-region reflective parameter identification algorithms, this method is used to identify the inflation pressure and load dependent parameters. Consequently, the model equations below were introduced to handle large inflation pressure changes. To regard the tyre inflation pressure p_i, the normalised change in inflation pressure dp_i is introduced.

$$dp_i = \frac{p_i - p_{i0}}{p_{i0}} \tag{6}$$

$$\mu_p = \mu_{px1} + \mu_{pVx1} + \mu_{pPx1} \cdot dp_i + \mu_{px2} \cdot df_z + \mu_{pPx2} \cdot dp_i^2 + \mu_{pPDx1} \cdot dp_i \cdot df_z + \mu_{px3} \cdot df_z^2 \tag{7}$$

$$\mu_S = \mu_{Sx1} + \mu_{SVx1} + \mu_{SPx1} \cdot dp_i + \mu_{Sx2} \cdot df_z + \mu_{SPx2} \cdot dp_i^2 + \mu_{SPSx1} \cdot dp_i \cdot df_z + \mu_{Sx3} \cdot df_z^2 \tag{8}$$

$$C_\lambda = C_{x1} + C_{Vx1} + C_{Px1} \cdot dp_i + C_{x2} \cdot df_z + C_{Px2} \cdot dp_i^2 + C_{PCx1} \cdot dp_i \cdot df_z + C_{x3} \cdot df_z^2 \tag{9}$$

Consequently, the inflation pressure dependent coefficients can be used to calculate the longitudinal force, respectively the longitudinal friction force coefficient, of the presented *HSRI* tyre model (c.f. equation (11-13)). The maximum friction coefficient at reference inflation pressure and reference load is considered according to equation (10) analogous to the extensions from *Ding* and *Taheri* [22].

$$\mu_{mod} = \mu_p - (\mu_p - \mu_S) \cdot \lambda \tag{10}$$

$$K_D = \frac{\mu_{mod} \cdot F_z \cdot (1 + \lambda)}{2 \cdot \sqrt{(C_\lambda \cdot \lambda)^2 + (C_\alpha \cdot \tan \alpha)^2}} \tag{11}$$

$$f(K_D) = \begin{cases} K_D(2 - K_D) & if \ K_D < 1 \\ 1 & if \ K_D \geq 1 \end{cases} \tag{12}$$

$$\mu_x = C_\lambda \cdot \frac{\lambda}{1 + \lambda} \cdot f(K_D) \tag{13}$$

To avoid extended tyre wear at very high slip values, the maximum slip of the test procedure was limited to 30% in this study. To consider this condition, the normalized slip λ_{norm} is

introduced and used instead of the slip λ. Therefore, the slip scale from 0 to 100% slip was divided by the desired slip limit λ_{end} of 0.3 according to equation (14). To avoid an influence on the slip stiffness C_λ, equation (9) must be multiplied by λ_{end} as well. Consequently, the coefficient of sliding friction is transferred to the new slip scale and allows a good fitting for this situation.

$$\lambda_{norm} = \frac{\lambda}{\lambda_{end}} \tag{14}$$

Table 3 presents the description of the coefficients that were used for the relations to describe the extension of the tyre model for large inflation pressure change.

Table 3: Used tyre model parameters with an example data set of the SUV tyre

Factor	Description	Example [-]
μ_{px1}	Static friction value μ_p at $F_{z,nom}$	1.6947
μ_{px2}	Variation of μ_p with load	-0.2376
μ_{px3}	Variation of μ_p with load squared	-0.0710
μ_{pPx1}	Variation of μ_p with tyre inflation pressure	0.3453
μ_{pPx2}	Variation of μ_p with tyre inflation pressure squared	-0.2161
μ_{PDx1}	Linear combination of pressure and load effects on μ_p	0.0639
μ_{pVx1}	Vertical offset factor of μ_p	-0.0078
μ_{Sx1}	Longitudinal shape factor μ_S at $F_{z,nom}$	1.1527
μ_{Sx2}	Variation of μ_S with load	0.0435
μ_{Sx3}	Variation of μ_S with load squared	-0.0908
μ_{SPx1}	Variation of μ_S with tyre inflation pressure	-0.1085
p_{SPx2}	Variation of μ_S with tyre inflation pressure squared	-0.1901
μ_{SPSx1}	Linear combination of pressure and load effects on μ_S	0.2237
μ_{SVx1}	Vertical offset factor of μ_S	-0.0070
C_{x1}	Longitudinal slip stiffness C_λ at $F_{z,nom}$	22.1132
C_{x2}	Variation of C_λ with load	-0.5666
C_{x3}	Variation of C_λ with load squared	6.3996
C_{Px1}	Variation of C_λ with tyre inflation pressure	-23.9078
C_{Px1}	Variation of C_λ with tyre inflation pressure squared	33.1528
C_{PCx1}	Linear combination of pressure and load effects on C_λ	-12.9296
C_{Vx1}	Vertical offset factor of C_λ	-0.8369

The combination of the basic parameters of the *HSRI* tyre model at reference inflation pressure and reference load with the inflation pressure and wheel load dependent parameters were handled in the presented tyre model with an introduced offset factor (e. g. μ_{pVx1}). Thus, the described parameter identification can be performed independently of the already determined reference point a limiting constraint of the model can be avoided. Consequently, the accuracy at the reference pressure and load is slightly reduced, but the overall fitting results can be improved significantly.

3.2.3 Fitting Results
Below, the results of the above described entire parameter identification process of the *HSRI* tyre model extended for large inflation pressure variations is presented for the SUV tyre as an example. Based on the introduced relations, the essential tyre properties can be computed for wheel load and inflation pressure changes. The parameterized model equations (illustrated as

surface plots) to calculate the longitudinal static friction force coefficient μ_p (cf. Figure 10 (left)), the longitudinal slip stiffness C_Kλ (cf. Figure 10 (right)) and the longitudinal sliding friction coefficient μ_s (cf. Figure 11) depending on tyre inflation pressure and load as well as the measured values the are shown in the illustrations below. Obviuosly, all studied parameters have a significant wheel load and tyre inflation pressure dependency. Although this is not presented, the trends also apply to the other analysed tyres.
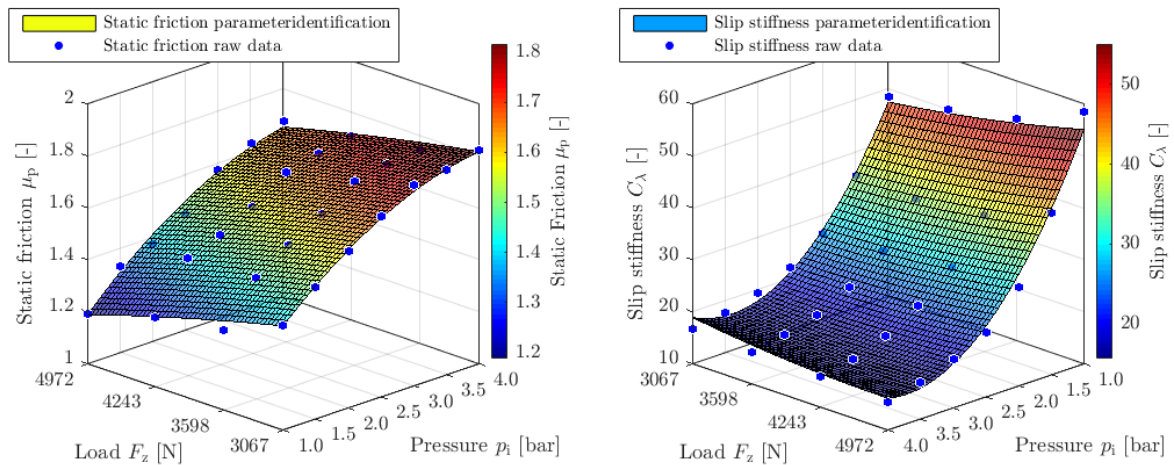

Figure 10: Inflation pressure and wheel load influences on static friction value μ_p (left) and slip stiffness C_λ (right): Simulated vs. measured data of SUV tyre
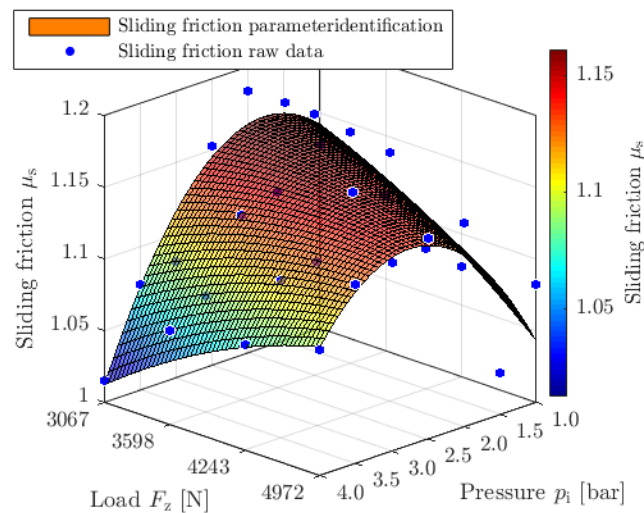

Figure 11: Inflation pressure and wheel load influences on sliding friction μ_s: Simulated vs. measured data of SUV tyre

Figure 12 presents the measured longitudinal friction force vs. brake slip characteristics as well as the curves obtained from the parameterized enhanced *HSRI* tyre model for a constant tyre inflation pressure of 2.5 bar. As expected, peak friction force coefficient and slip stiffness increase with a decreasing load. As illustrated, the different friction force coefficient vs. brake slip characteristic curves are represented, also at low and high wheel loads, precisely by the parameterized tyre model.
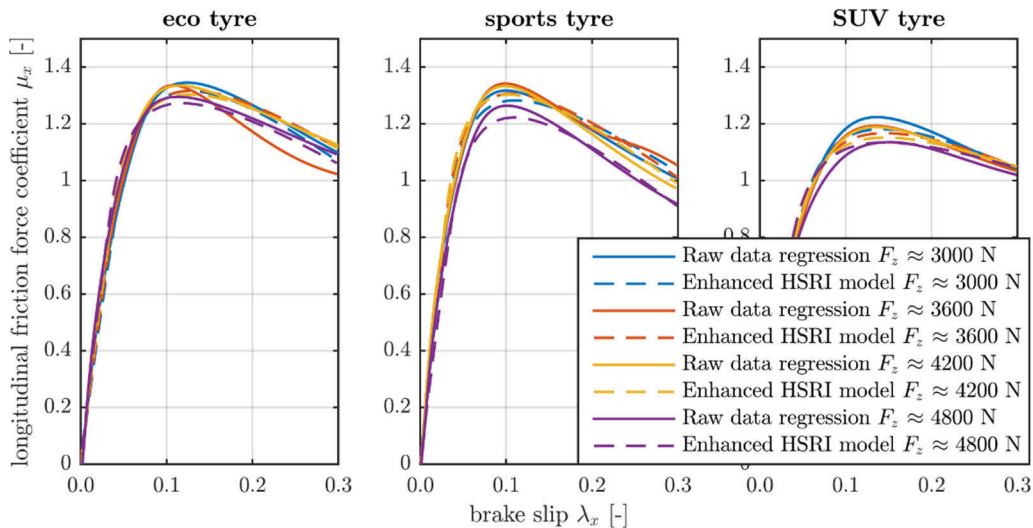
Figure 12: Wheel load influence on the friction force coefficient vs. brake slip tyre characteristic curve of three analysed tyres – simulated with the enhanced HSRI tyre model.

Figure 13 presents the friction force coefficient vs. brake slip tyre characteristic curves of the three tyres for different inflation pressures at a constant wheel load of about 3000 N. As described above, the individual measurement curves are represented very well by the extended *HSRI* tyre model. Even at low as well as high tyre inflation pressures the model accuracy can be regarded as very satisfying.
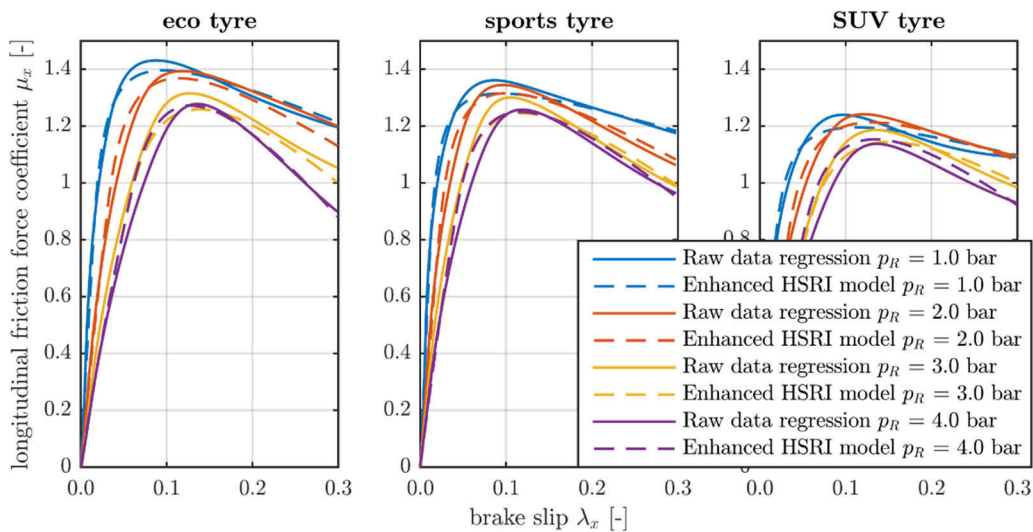

Figure 13: Inflation pressure influence on the friction force coefficient vs. brake slip tyre characteristic curve of three analysed tyres - simulated with the enhanced HSRI tyre model

Subsequently, it can be noted that the measured tyre characteristics are represented very well by the presented extensions to improve the *HSRI* tyre model. Due to the introduced enhancements the tyre simulation model can be used for large inflation pressure variations. To quantify the deviation between the measured and modelled tyre characteristics, the fit error ε, which is obtained according to eq. (15), is used. In this equation *i* denotes each sample point of the friction coefficient curves and *n* is the total number of sample points. The subscripts *Model* and *Measurement* describe the fit results of the enhanced tyre model and the measurement results.

$$\varepsilon = \sqrt{\frac{\sum_{i=1}^{n}\left(\mu_{Model,i} - \mu_{Measured,i}\right)^2}{\sum_{i=1}^{n}\left(\mu_{Measured,i}\right)^2}} \tag{15}$$

The parameters of the enhanced tyre model were identified from measurements with a large variation of operation points. Especially, the inflation pressure was varied from 1.0 bar to 4.0 bar in 0.5 bar steps for every analysed tyre. For every operation point, and consequently for every individual tyre characteristic curve, the fitting error between the fitted tyre model and the measured results were calculated.

Table 4: Overview fit-error values of the enhanced HSRI model

Fit-error	Model	Corner 48" sports tyre	Corner 48" eco tyre	Corner 48" SUV tyre
Lowest	*MF* **v2012**	4.21 %	2.09 %	2.72 %
	Enhanced *HSRI*	3,31 %	2,84 %	3,32 %
Highest	*MF v***2012**	12.65 %	16.04 %	7.25 %
	Enhanced *HSRI*	5,75 %	12,26 %	7,24 %
Average	*MF* **v2012**	7.10 %	6.06 %	4.40 %
	Enhanced *HSRI*	4,20 %	4,92 %	4,19 %

To evaluate the model accuracy, the fitting results of the enhanced *HSRI* tyre model are compared with the fitting results of the well-known (wheel load and tyre inflation pressure dependent) *Magic Formula* v2012 tyre model. Table 4 presents the lowest, highest and mean fit error for the fitted tyre characteristics for all analysed loads and tyre inflation pressures. The improvement of the model quality is shown throughout. It can be seen that the average fitting accuracy for all analysed tyres are slightly better with the presented tyre model. The benefit of the model becomes particularly clear by looking at the highest fit error. These values reflect the fitting results at higher and lower tyre inflation pressures. The mean value of the highest fit errors (for the three analysed tyres) decrease from around 11.98 % (*Magic Formula* v2012) to about 8.41 % using the enhanced *HSRI* tyre model. Subsequently, the fitting results confirm that the enhanced tyre model presented in this publication increases the model accuracy significantly for large tyre inflation pressure variations. Consequently, the tyre model can i. a. be used to simulate the potential of an integrated highly dynamic Tyre Pressure Control System (TPCS) on vehicle dynamics.

4. SUMMARY AND OUTLOOK

Using the Corner Module Test Rig (CMTR) recently developed by the *Automotive Engineering Group* at *Technische Universität Ilmenau*, a large variation of inflation pressure and load variations on longitudinal tyre characteristics were analysed for three different tyres. The results illustrate a distinct influence of load and especially tyre inflation pressure. Hence, the *HSRI* tyre model has been extended for large inflation pressure and wheel load variations. A comparison with the well-known *Magic Formula v2012* tyre model, which considers small inflation pressure variations, demonstrates a good model accuracy of the enhanced *HSRI* tyre model.

The enhanced tyre model will be implemented to an *IPG CarMaker* multi-body vehicle model. Using the numerical vehicle dynamics simulation tool in co-simulation with *LMS AMESim* to simulate a pneumatic Tyre Pressure Control System (TPCS) and *MATLAB Simulink* to represent

the control unit, a comprehensive analytical study will be performed to quantify the benefits of a TPCS on different types of vehicles. This will be part of a next publication of the authors.

In addition to the presented results that were extracted from experiments performed on the smaller 48" test rig drum of the chassis roller dynamometer, studies on the larger 75" drum were carried out. Moreover, a Tyre Test Trailer was recently developed at the *Automotive Engineering Group* at *TU Ilmenau* to analyse the effect of inflation pressure variations on tyre characteristics under dry and wet real road conditions. First results show quantitative differences between the measurements realized on real roads and laboratory surfaces with different curvatures. This will be discussed in a next paper of the authors.

REFERENCES

[1] Pruckner, A., Ochner, U., Eiletz, R., König, R., „Ein hocheffizientes Fahrwerk für ein hocheffizientes Konzeptfahrzeug", 15. Internationale VDI-Tagung Reifen-Fahrwerk-Fahrbahn 2015, VDI-Berichte Nr. 2241, ISBN 978-3-18-092241-6.

[2] Strübel, C., Wies, B., Ochs, M., „Potenzial für Rollwiderstandsverbesserung durch neue Reifendimensionen", 15. Internationale VDI-Tagung Reifen-Fahrwerk-Fahrbahn 2015, VDI-Berichte Nr. 2241, ISBN 978-3-18-092241-6.

[3] Michelin Reifenwerke KGaA (Hrsg.), „Der Reifen: Rollwiderstand und Kraftstoffersparnis", Société de Technologie Michelin, ISBN 2-06-711658-4, Deutsche Erstauflage, 2005.

[4] Clark, S. K. and Dodge, R.N., "A Handbook for the Rolling Resistance of Pneumatic Tires", Industrial Development Division, Institute of Science and Technology, The University of Michigan, Ann Arbor, USA, 1979.

[5] Wong, J.Y., "Theory of Ground Vehicles", John Wiley & Sons, 2008, ISBN: 978-0470170380.

[6] Glaeser, K.P., Zöller, M, „Der Rollwiderstand von Reifen auf Fahrbahnen", 3. Symposium Reifen und Fahrwerk 2005, VDI Reihe 12 Nr. 603, ISBN: 3-18-360312-8.

[7] National Research Council, „Tires and passenger vehicle fuel economy: Informing consumers, improving performance", Washington, DC: Transportation Research Board, 2006, ISBN: 0309094216.

[8] Hadrys, D., Wegrzyn, T., and Miros, M., "The Influence of various pressures in pneumatic tire on braking process of car with anti-lock braking system", Transport Problems, 2008.

[9] Marshek, K., Cuderman, J., and Johnson, M., "Performance of Anti-Lock Braking System Equipped Passenger Vehicles - Part III: Braking as a Function of Tire Inflation Pressure," SAE Technical Paper 2002-01-0306, 2002, doi:10.4271/2002-01-0306.

[10] National Highway Traffic Safety Administration (NHTSA), "Tire Pressure Monitoring System FMVSS No. 138", Final Regulatory Impact Analysis, Washington DC, USA: U.S. Department of Transportation, 2005.

[11] Höpping, K. and Augsburg, K., "Dynamic Tire Pressure Control System - Analysis of the effect on longitudinal vehicle dynamics and fuel consumption", Shaping the future by engineering: 58th IWK, Ilmenau Scientific Colloquium, Proceedings, Ilmenau, 8 - 12 September 2014. Ilmenau, Germany:ilmedia.

[12] Höpping, K., Augsburg, K., Hutengs, K., Dherbomez, G. et al., "Analysis of the effect of tire inflation pressure on tire road interaction during braking", The Dynamics of Vehicles on Roads and Tracks, Proceedings of the 24th Symposium of the International Association for Vehicle System Dynamics (IAVSD 2015), Graz, Austria, 17-21 August 2015, CRC Press 2016, p. 731–737, doi: 10.1201/b21185-79.

[13] Savitski, D., Höpping, K., Ivanov, V., and Augsburg, K., "Influence of the Tire Inflation Pressure Variation on Braking Performance of Full-Electric Vehicle with Continuous Anti-Lock Braking System", SAE Technical Paper 2015-01-0643, 2015, doi: 10.4271/2015-01-0643.

[14] Munro, R., MacCulloch F., "Tyre Pressure Control on Timber Haulage Vehicles: Some observations on a trial in Highland, Scotland", Final Report ROADEX III, 2008.

[15] Skoff, G. "Automatische Luftdruck Regelung ALR: Ein umfassender Beitrag für das Automobil der Zukunft", 3. Symposium Reifen und Fahrwerk 2005, VDI Reihe 12 Nr. 603, ISBN: 3-18-360312-8.

[16] Augsburg, K., Ivanov, V., Kruchkova, K., Höpping, K. et al.,"Project Adtyre: Towards Dynamic Tyre Inflation Control", Proceedings of the FISITA 2012 World Automotive Congress, Lecture Notes in Electrical Engineering, vol 198, Berlin, Heidelberg: Springer, doi 10.1007/978-3-642-33795-6_16.

[17] Halfmann, C., Holzmann, H., „Adaptive Modelle für die Kraftfahrzeugdynamik", Berlin, Heidelberg: Springer, 2003, ISBN: 3642182151.

[18] Uil, R. T. "Tyre models for steady-state vehicle handling analysis". Master thesis, DCT 2007.142. TU Eindhoven, 2007.

[19] Bösch, P., Ammon, D., Klempau, F., "Reifenmodelle -Wunsch und Wirklichkeit aus der Sicht der Fahrzeugentwicklung". In: 4. Darmstädter Reifenkolloquium, Fortschritt-Berichte VDI Reihe 12, Nr. 511 (2002), p. 87–101.

[20] Höpping, K., Augsburg, K., Büchner, F., " Vergleich des Reifenfülldruckeinflusses auf Reifenkennlinienmessungen unter Labor- und Realbedingungen ", In: 16. Internationale VDI-Tagung „Reifen-Fahrwerk-Fahrbahn", Hannover, 25.-26.10.2017.

[21] Doumiati, M., Charara, A., Victorino, A., and Lechner, D., "Vehicle dynamics estimation using Kalman filtering: Experimental validation. Automation-control and industrial engineering series", London: Iste, 2012. ISBN: 1118579003.

[22] Ding, N. and Taheri, S. "A Modified Dugoff Tire Model for Combined-slip Forces". In: Tire Science and Technology 38.3, p. 228–244, 2010, doi: 10.2346/1.3481696.

[23] Wang, B., Qi, C., Victorino, A., and Charara, A. "Real-time experimental validation of nonlinear observer for vehicle dynamics parameters estimation: A laboratory vehicle description". In: 2012 IEEE International Conference on Vehicular Electronics and Safety (ICVES 2012), Istanbul, Turkey, p. 72–77, 2012, doi: 0.1109/ICVES.2012.6294286.

[24] Wang, B., Victorino, A., Charara, A., Augsburg, K., and Höpping, K. "Assessment of rollover stability based on risk indicator". In: 2013 IEEE Symposium on Computational Intelligence for Engineering Solutions (CIES), Singapore, S. 56-60, 2013, doi: 10.1109/CIES.2013.6611729.

[25] Bian, M., Chen, L., Luo, Y., and Li, K., "A Dynamic Model for Tire/Road Friction Estimation under Combined Longitudinal/Lateral Slip Situation", SAE Technical Paper 2014-01-0123, 2014, doi:10.4271/2014-01-0123.

[26] Ding, N., and Taheri, S., "A Modified Dugoff Tire Model for Combined-slip Forces", Tire Science and Technology, TSTCA, Vol. 38, No. 3, p. 228-244, 2010, doi: 10.2346/1.3481696.

[27] Villagra, Jorge, Brigitte d'Andrea Novel, Michel Fliess, and Huges, Mounier: "A diagnosis-based approch for tire-road forces and maximum friction estimation." Control Engineering Practice, 19: p. 174-184, 2011, doi: 10.1016/j.conengprac.2010.11.005.

[28] He, R., Jimenez, E., Savitski, D., Sandu, C., Ivanov, V., "Investigating the Parameterization of Dugoff Tire Model Using Experimental Tire-Ice Data," SAE Int. J. Passeng. Cars - Mech. Syst. 10(1):83-92, 2017, doi: 10.4271/2016-01-8039.

[29] van Oosten, J J.M, Unrau, H.-J., Riedel, A., and Bakker, E., "TYDEX Workshop: Standardisation of Data Exchange in Tyre Testing and Tyre Modelling", Vehicle System Dynamics, Volume 27, 1997, p. 272-288, doi: 10.1080/00423119708969660.

[30] Carlson, C. R.; Gerdes, J. C., „Identifying Tire Pressure Variation by Nonlinear Estimation of Longitudinal Stiffness and Effective Radius", Proceedings of AVEC '02, 6th International Symposium on Advanced Vehicle Control, 9.-13. September 2002, Hiroshima, Japan.

[31] Zegelaar, P.W.A., "The dynamic response of tyres to brake torque variations and road unevennesses", PhD thesis Delft University of Technology, The Netherlands, 1998, ISBN: 90-370-0166-1.

[32] Dugoff, H, Fancher. P. S., and Segel, L., "Tire performance characteristics affecting vehicle response to steering and braking control inputs". Final Report. Ann Arbort, Michigan, USA: Highway Safety Research Institute, The University of Michigan, 1969.

[33] Bernard, J. E., Segel, L., Wild, R.E., "Tire shear force generation during combined steering and braking maneuvres", SAE Paper 770852, 1977.

[34] Wiegner, P., "Über den Einfluss von Blockierverhinderern auf das Fahrverhalten von Personenkraftwagen bei Panikbremsungen", Dissertation, Technische Universität Braunschweig, 1974.

[35] Uffelmann, F., "Berechnung des Lenk- und Bremsverhaltens von Kraftfahrzeugzügen auf rutschiger Fahrbahn", Dissertation, Technische Universität Braunschweig, 1980.

[36] Bian, M., Chen, L., Luo, Y., and Li, K., "A Dynamic Model for Tire/Road Friction Estimation under Combined Longitudinal/Lateral Slip Situation", SAE Technical Paper 2014-01-0123, 2014, doi:10.4271/2014-01-0123.

[37] Schramm, D., Hiller, M., Bardini, R., "Vehicle Dynamics: Modeling and Simulation", Berlin Heidelberg: Springer, 2014, ISBN: 9783540360452.

[38] Mitschke, M., Wallentowitz, H., "Dynamik der Kraftfahrzeuge", 5. Aufl., Berlin Heidelberg: Springer, 2014, ISBN: 9783658050689.

[39] Gim, G. "Vehicle dynamic simulation with a comprehensive model for pneumatic tires". Dissertation. The University of Arizona, USA, 1988.

[40] van Oosten, J J.M. and Bakker, E., "Determination of Magic Tyre Model Parameters", Vehicle System Dynamics, 21:S1, 1992, p. 19-29, doi: 10.1080/00423119208969995.

[41] Schuring, D., Pelz, W., and Pottinger, M., "The BNPS Model - An Automated Implementation of the "Magic Formula" Concept", SAE Technical Paper 931909, 1993, doi:10.4271/931909.

[42] Cabrera, J. A., Ortiz, A., Carabias, E., and Simon. A., "An Alternative Method to Determine the Magic Tyre Model Parameters Using Genetic Algorithms", Vehicle System Dynamics, Volume 41, 2004, doi: 10.1076/vesd.41.2.109.26496.

[43] Ortiz, A., Cabrera, J. A., Guerra, A. J., and Simon. A., "An easy procedure to determine Magic Formula parameters: a comparative study between the starting value optimization technique and the IMMa optimization algorithm", Vehicle System Dynamics, Volume 44, 2006, p. 689-718, doi: 10.1080/00423110600574558.

[44] Vijay Alagappan, A. Narasimha Rao, K. V., and Krishna Kumara, R., "A comparison of various algorithms to extract Magic Formula tyre model coefficients for vehicle dynamics simulations", Vehicle System Dynamics, Volume 53, 2014, p. 154-178, doi: 10.1080/00423114.2014.984727.

[45] The MathWorks., "Optimization Toolbox User's Guide", Natick, USA, 2016.

[46] Hoogh, J. de. "Implementing inflation pressure and velocity effects into the Magic Formula tyre model", master thesis, DCT Rep. 2005.46, Eindhoven University of Technology, the Netherlands, 2005.

[47] Schmeitz, A. J. C., Besselink, I. J. M, Hoogh, J. de, and Nijmeijer,H., "Extending the Magic Formula and SWIFT tyre models for inflation pressure changes". Fahrwerk, Reifen, Fahrbahn, VDI Berichte Nr. 1912, 2005, p. 201-225.

[48] Veld, I. o. h., "Enhancing the MF-Swift tyre model for inflation pressure changes", master thesis, DCT Rep. 2007.144, Eindhoven University of Technology, the Netherlands, 2007.

[49] Besselink, I. J., Schmeitz, A. J., and Pacejka, H. B. "An improved Magic Formula/Swift tyre model that can handle inflation pressure changes", Vehicle System Dynamics, Volume 48, 2010, p. 337–352.

[50] Pacejka, H., "Tire and Vehicle Dynamics", 3rd Edition, Butterworth-Heinemann, 2012, ISBN 978-0080970165.

[51] Schmeitz, A. J. C., Leneman, F., "MF-Tyre/MF-Swift 6.1.1", Help Manual, TNO Automotive, Helmond, 2008.

[52] Schmeitz, A. J. C., „MF-Tyre/MF-Swift", The Future of Tire Technology 2013, Charlotte, USA, 28.-30.10.2013.

CONTACTS

Dipl.-Ing. K. Höpping   kristian.hoepping@tu-ilmenau.de